令和 4 年 7 月修士論文要旨

（東京大学大学院　新領域創成科学研究科　海洋技術環境学専攻）

Experimental study of the motion of aircushion type platform in waves focusing on the inner free surface

（内部自由表面に着目したエアクッション浮体の波浪中動揺に関する実験的研究）

学籍番号 47-206778　　何　億寧 (He Yining)
指導教員　　平林　紳一郎　准教授

(令和 4 年 7 月 29 日発表予定)
Keywords: エアクッション浮体，実験研究，空気室内自由表面の計測，数値シミュレーション
Keywords: Aircushion type platform, experimental study, inner free surface measurement, numerical simulation

1. INTRODUCTION

As a way to reduce global carbon emissions, offshore wind has become increasingly important in recent years to the future. Many types of floating platforms could be used as FOW platforms [1].

In recent years, aircushion-supported platforms have been investigated and used for practice. One of the prominent features of the aircushion platform is that it contains the inner free surface, which is related to the buoyancy, wave excitation, inner pressure variation and so on, which contributes to the hydrodynamic and hydroelastic performance [2]. It is of great importance to research the inner free surface of the aircushion platform. Some theories related to the inner water elevation have been studied and proposed as well as numerical simulations [3]. However, few researchers have measured the inner wave field experimentally.

In this study, for the purpose of measuring and analyzing the inner free surface elevation in various incident regular wave conditions, two kinds of aircushion models are tested in moored and fixed conditions, and the inner free surface elevations along the inner aircushion chamber were measured. The coupling effects between the inner free surface elevation and the motion responses of aircushion models have been discussed. The experimental results are compared with the numerical simulation results of WAMIT [4] as well.

2. THEORY AND METHOD

2.1 The stability of aircushion platform

According to [5], the $\overline{KM}$ value (the distance between the bottom and the metacenter of the platform) of the mono aircushion platform can be obtained by the following equation:

$$\overline{KM} = W + \frac{1}{2}T - TR\theta^2 + \cdots \tag{2.1}$$

$$R = \frac{H}{\kappa(T + P_0/\rho g)} \tag{2.2}$$

here, θ is the heel angle.

2.2 Compressibility of the aircushion

The compressibility factor ε of the aircushion, which is proposed by van Kessel [6], is presented as follows:

$$\varepsilon = \frac{\rho g H}{\rho g T + P_o + \rho g H} = \frac{H}{T + H + \frac{P_0}{\rho g}} \tag{2.3}$$

here, ρ is the water density, g is acceleration due to gravity, H is the height of aircushion, T is the difference between the inner and outer water surface, P_o is atmospheric pressure.

2.3 The Marker-Net method

The Marker-Net method (MNM) was proposed by Mozumi et al. [7], which can be used to visualize the water surface. The Marker-Net is consisted of several floats and a flexible net. The floats are attached in a grid to the net floating on the water surface. The motions of the floats are captured by the cameras at the same time, then the coordinates of the floats are determined. The feasibility and effectiveness of using the Marker-Net to reconstruction the wave field are validated in [7] and [8].

3. MODEL TESTS

For the purposes of analyzing the coupling effect between the model motion and the inner free surface elevation, measuring the inner free surface elevation working as the database that could be used to compare with the numerical simulation, model tests had been done at the Experimental tank in the University of Tokyo.

3.1 Experimental condition

Three kinds of models, rectangular barge type model, mono aircushion type model and partitioned aircushion type model, with the same dimensions have been tested in the experiment. Two types of arrangements of the moored condition and the fixed condition were tested as shown in Fig.1.

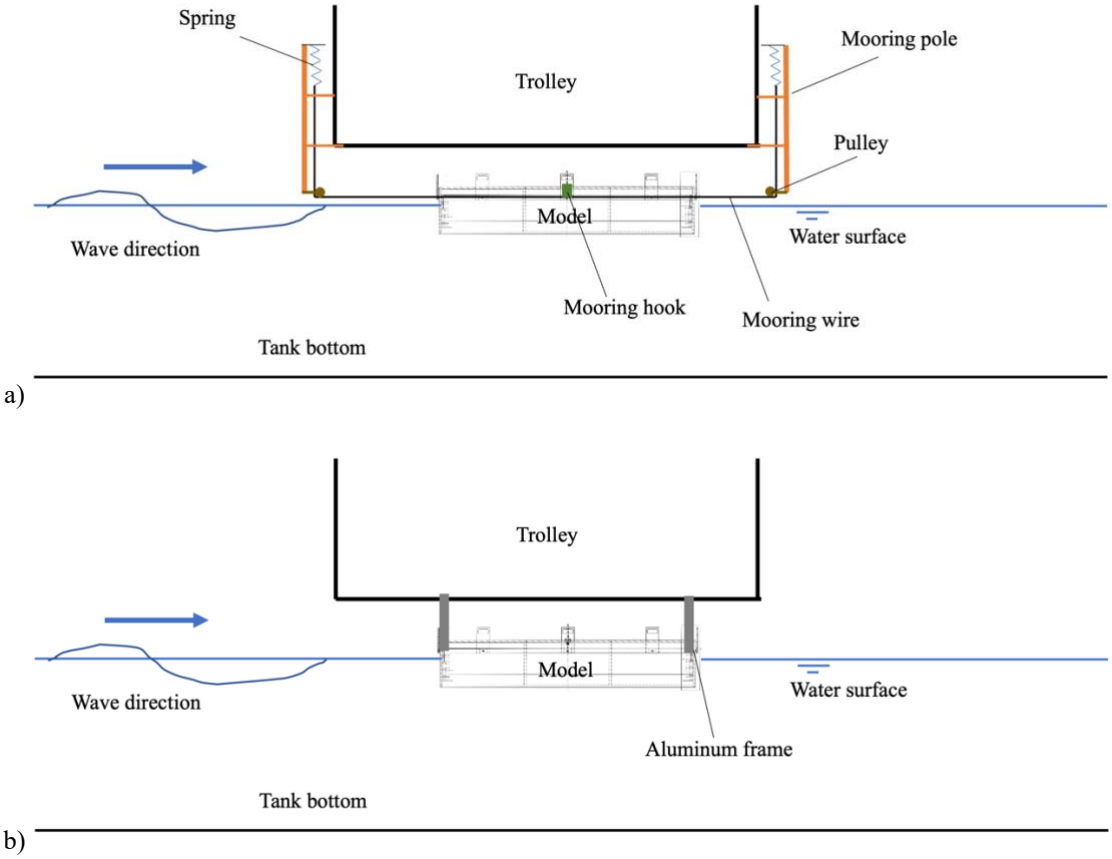

Fig. 1. Arrangement of the model in (a) moored condition, and (b) fixed condition.

3.2 Measurement of inner water elevation

The inner free surface elevations along the aircushion chamber are measured by Marker-Net method, which is proposed by Mozumi et al [5] and validated by Houtani et al [6]. Foamed polystyrene balls with a diameter of 15 mm are wrapped in an infrared reflective film that could be tracked by the Qualisys infrared cameras. The balls are fixed to a soft net with an interval of 50 mm, as can be seen in Fig.2.

The balls and the net are very soft and light so they can float on the water surface and barely influences the motions of the water surface in regular waves. The size of the balls should be carefully chosen, they should be tracked effectively by the Qualisys cameras and meanwhile, they do not interfere with each other.

4. RESULTS AND DISCUSSION

4.1 Free decay test

The heave natural period of the mono aircushion type model is almost the same as that of the partitioned aircushion type and slightly larger than that of the barge type model. The pitch natural period is increased by the models with aircushion, while the natural period of the partitioned aircushion model is closer to that of the barge type model.

4.2 Regular wave test

The results of heave and pitch motion responses are shown in Fig.3. The heave motion responses of the three kinds of models are almost the same. Especially for the aircushion type models, “no-wave-point” seems to occur when λ/L (λ stands for the wavelength) equals 0.5 and 1 for the two kinds of aircushion models and λ/L equals 1.5 only for the partitioned aircushion model.

In the wave condition that $\lambda/L < 2$, the pitch motion response of the mono aircushion model is the smallest. The pitch motion responses of the partitioned aircushion model are similar to that of the barge type model, while in the wave condition that $\lambda/L < 1.2$ the motion response is smaller and vice versa.

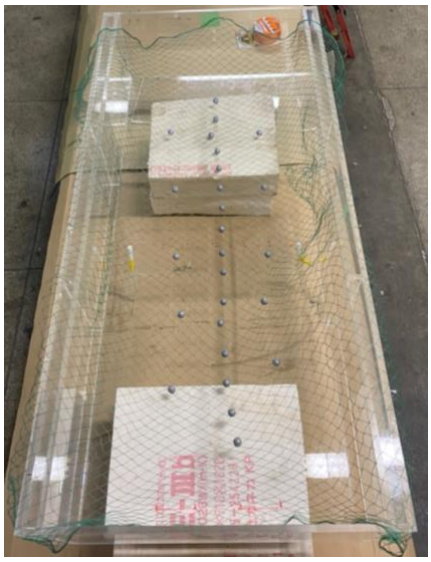

Fig.2. A photo of the aircushion model with marker net.

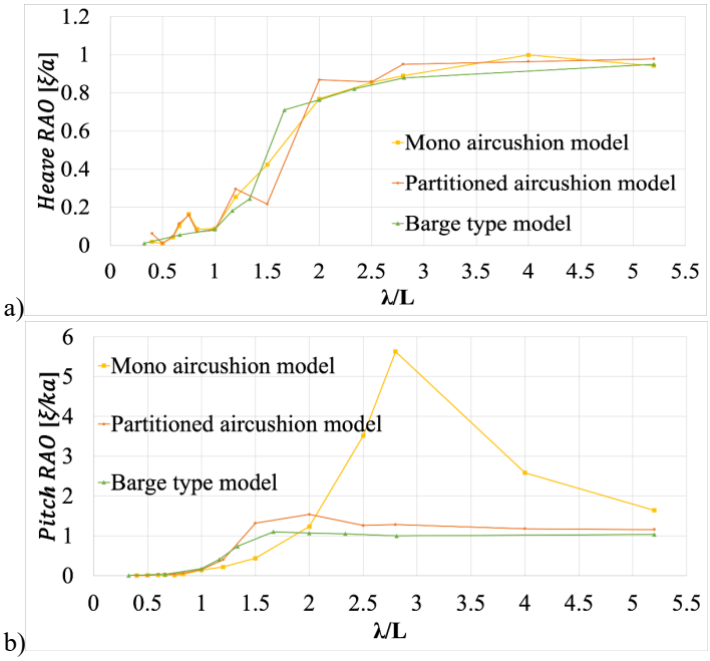

Fig.3. Motion responses of models, (a) heave, and (b) pitch.

4.3 Inner free surface elevation

Mono aircushion model in moored condition.

When the wavelength condition λ/L is not larger than 0.75, as the Fig.4 (a). shows, the wave field is characterized by a complete standing wave. When λ/L is greater than 0.75 and less than 2, the wave field is characterized by a transit phase from a complete standing wave to a progressing wave. When λ/L is greater than 2, the inner free surface moves like a piston that the nondimensional amplitudes of the free surface are all about 1, as can be seen in Fig.4 (b).

Mono aircushion model in fixed condition.

When λ/L is less than 0.75, the wave field is characterized by a complete standing wave. When λ/L is greater than 0.75 and less than 2, the wave field is characterized by a transit phase from a complete standing wave to a sloshing wave. When λ/L is greater than 2, the inner wave field changes to a complete sloshing wave, very different from the model in the moored condition that shows the piston phenomenon.

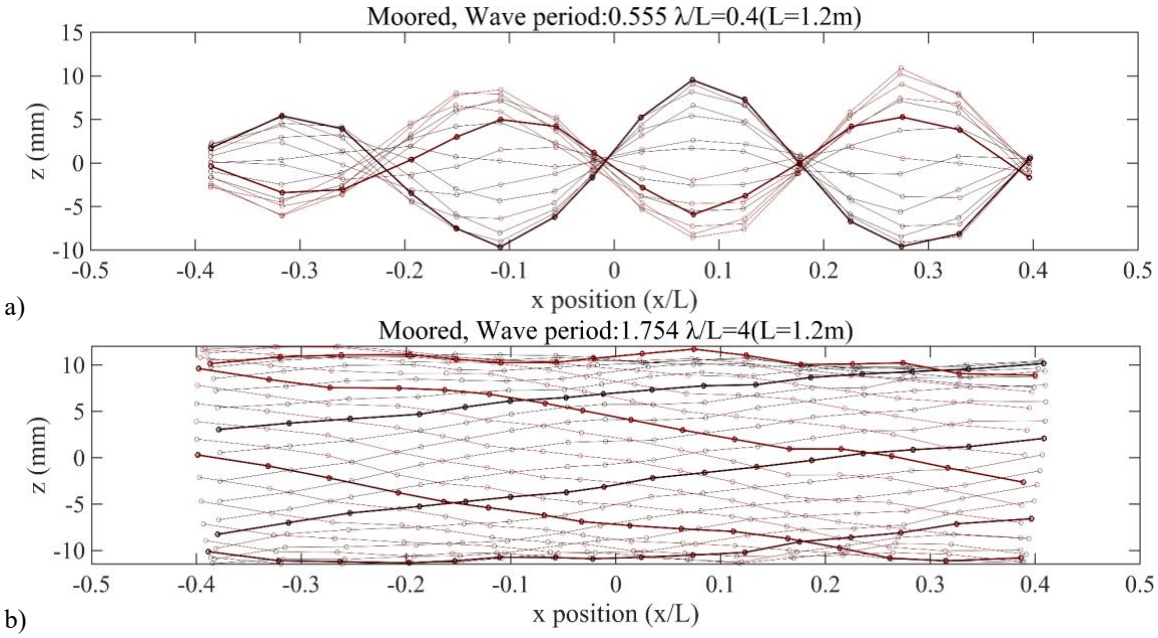

Fig.4. Inner surface elevation of mono aircushion model in moored condition, (a) $\lambda/L = 0.4$, and (b) $\lambda/L = 4$.

Partitioned aircushion model in moored condition.

When $\lambda/(L/2)$ is less than 1, (because the length of the aircushion chamber is $L/2$ for the partitioned aircushion model), the wave field is characterized by a complete standing wave. With the increasing of incident wavelength, the inner wave field changes to a sloshing wave and then to progressing wave, while for the model in the fixed condition, the inner wave field changes from a complete standing wave to a completed sloshing wave.

4.4 Results of numerical simulation

Numerical models of the mono aircushion model and partitioned aircushion model with the same dimension have been made and the inner surface elevations of the fixed condition have been calculated by WAMIT.

The results of WAMIT show some consistency with the experimental measurement, for the mono aircushion model, the wave fields are all standing waves when λ/L is less than 0.75, as shown in Fig.5 (a). However, with the increasing of incident wavelength, the inner wave fields firstly change to sloshing waves and then changes to progressing waves, as shown in Fig.5 (b). The same as partitioned aircushion model, in short wavelength conditions, the simulation results show the standing waves and sloshing waves, while for the long wavelength condition, wave fields change to progressing waves.

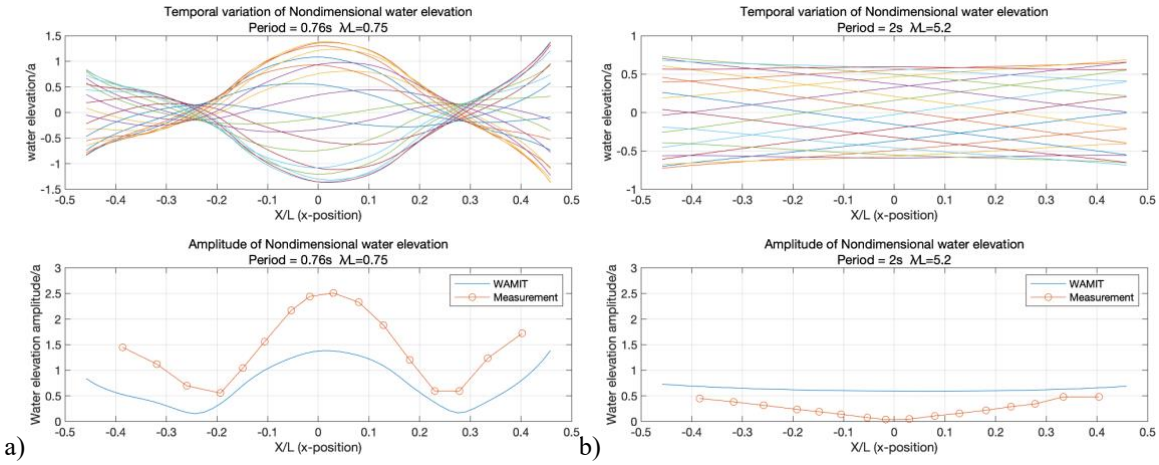

a) b)

Fig.5. Calculated result of inner surface elevation of mono aircushion model in fixed condition, (a) $\lambda/L = 0.75$, and (b) $\lambda/L = 5.2$.

5. CONCLUSION

In this study, according to the measurement of motion response and the inner free surface elevation of the three types of models as well as the inner free surface simulation by WAMIT, the following conclusions could be drawn.

- The inner wave fields of aircushion type platforms are standing waves for the incident wave with a short wavelength compared with the floater length, and, as the wavelength increases, they change to progressive waves or sloshing waves depending on the mooring condition of the platforms.
- Pitch motion responses of the mono aircushion platform are the smallest in the short wavelength condition, while the resonance motions occur in long wavelength condition. A peak of heave motion responses occurs while the inner free surface moves significantly, which is assumed to be related to the pressure change in the aircushion chamber.
- The inner free surface elevation of aircushion type models simulated by WAMIT was comparable with the experimental results for the short wavelength conditions while a large discrepancy was found for the long wavelength conditions.

Reference

[1] Expectation and Foresight of FOW in Japan Key for decarbonization in Japan. Japan's Floating Offshore Wind Group.

[2] Ikoma T, Maeda H, Masuda K, et al. Effects of the Air-chambers on the Hydroelastic Response Reduction. *Proceedings of International Symposium on Ocean Space Utilization Technology*, 2003, pg. 180-188.

[3] J.A.Pinkster, E.J.A.Meevers Scholte, The behaviour of a large air-supported MOB at sea, Marine Structure, vol 14-1-2, pg. 163-179, 2001.

[4] Lee, C.H. and Newman, J.N. (2013) WAMIT User Manual, Versions 7.4. WAMIT, Inc., Cambridge, MA

[5] "浮体の復原性について," SRC News:The Ship Research Centre of Japan, no. No.49, p. 6, Jan. 2001.

[6] J. L. F. van Kessel, "Aircushion supported mega-floaters.," [s.n.], S.l., 2010. ISBN: 9789085704966
OCLC: 840424819

[7] K. Mozumi, T. Waseda, and A. Chabchoub, "3D Stereo Imaging of Abnormal Waves in a Wave Basin," in *Volume 3: Structures, Safety and Reliability*, St. John's, Newfoundland, Canada, May 2015, p. V003T02A027. doi: 10.1115/OMAE2015-42318.

[8] H. Houtani, T. Waseda, and K. Tanizawa, "Measurement of spatial wave profiles and particle velocities on a wave surface by stereo imaging –validation with unidirectional regular waves–," *Journal of the Japan Society of* Naval Architects and Ocean Engineers, vol. 25, pp. 93–102, Sep.